Symmetries in human brain language pathways correlate with verbal recall

Marco Catani*†‡§, Matthew P. G. Allin†, Masud Husain¶, Luca Pugliese*, Marsel M. Mesulam‖, Robin M. Murray†, and Derek K. Jones**

*Section of Brain Maturation, †Department of Psychological Medicine, and ‡Centre for Neuroimaging Sciences, Institute of Psychiatry, King's College London, London SE5 8AF, United Kingdom; ¶Institute of Cognitive Neuroscience, University College London, London WC1N 3AR, United Kingdom; ‖Northwestern University, 320 East Superior Street, 11-450, Chicago, IL 60611; and **Cardiff University Brain Research Imaging Centre, School of Psychology, Cardiff University, Cardiff CF10 3AT, United Kingdom

Edited by Fernando Nottebohm, The Rockefeller University, Millbrook, NY, and approved September 7, 2007 (received for review March 7, 2007)

Lateralization of language to the left hemisphere is considered a key aspect of human brain organization. We used diffusion tensor MRI to perform *in vivo* virtual dissection of language pathways to assess the relationship between brain asymmetry and cognitive performance in the normal population. Our findings suggest interhemispheric differences in direct connections between Broca's and Wernicke's territories, with extreme leftward lateralization in more than half of the subjects and bilateral symmetrical distribution in only 17.5% of the subjects. Importantly, individuals with more symmetric patterns of connections are better overall at remembering words using semantic association. Moreover, preliminary analysis suggests females are more likely to have a symmetrical pattern of connections. These findings suggest that the degree of lateralization of perisylvian pathways is heterogeneous in the normal population and, paradoxically, bilateral representation, not extreme lateralization, might ultimately be advantageous for specific cognitive functions.

arcuate fasciculus | brain asymmetry | diffusion tensor imaging | language lateralization | verbal memory

One of the most distinctive features of the human brain is the asymmetric distribution of cognitive functions between the two hemispheres, generally referred to as lateralization (1). Although the behavioral correlates of structural asymmetry described in other animals remain to be clarified (2, 3), in humans, left–right differences have been linked to the development of language (4). Evidence for specialization of the human left hemisphere for language derives from lesion, functional, and structural anatomical findings (1, 4–9).

The most compelling evidence for language lateralization comes from studies of patients with language deficits after brain lesions. In right-handed adults presenting with aphasia, the brain lesion is almost invariably located in the left hemisphere (1, 5). Similar prevalence data have been found in subjects undergoing brain surgery for epilepsy, with lateralization of language to the left hemisphere being observed in >90%, but not all, of the right-handed subjects (7, 9, 10). The structural correlates of language lateralization are less clear. In their original paper, Geschwind and Levitsky (4) found an asymmetry of the size of the planum temporale, a region of the temporal lobe belonging to Wernicke's territory, in 65% of the population. However, Dorsaint-Pierre *et al.* (10) have recently found that the leftward lateralization of the planum temporale does not correlate with language lateralization as assessed by the sodium amytal procedure. On the other hand, several studies have reported a higher prevalence of leftward asymmetry of perisylvian white matter volumes, suggesting that language networks represent a more likely anatomical substrate for lateralization of language functions rather than cortical areas alone (11–14). However, the behavioral correlates of lateralization of white matter pathways remain unknown.

Despite this extensive research, it remains unclear whether language abilities actually relate to the degree of brain asymmetry (7, 10). Indeed, recent studies show that the right hemisphere may contribute to some aspects of language function, such as semantic processing (15, 16), word learning (17), and retrieval (18, 19).

Here we used diffusion tensor (DT) MRI (DT-MRI) tractography to examine the asymmetry of perisylvian language pathways and behavioral correlates. DT-MRI tractography is a noninvasive technique that, instead of visualizing axons directly, reconstructs their trajectories by measuring the diffusivity of water along different directions and tracing a pathway of least hindrance to diffusion (parallel to the dominant fiber orientation) to form continuous pathways. DT-MRI facilitates the study of large-scale brain networks, including those subserving language (11–13, 20–22). Recent DT-MRI investigations have revealed three important parts of the language network (21). First, there is the well established direct pathway (21) connecting Wernicke's territory in the left temporal lobe with Broca's territory in the left frontal lobe through the arcuate fasciculus (11–13, 20–22). In addition, there is an indirect pathway (21) consisting of two segments, an anterior segment linking Broca's territory with the inferior parietal lobe (Geschwind's territory) (21), and a posterior segment linking Geschwind's territory with Wernicke's territory (13, 20, 21). Not only does this arrangement support the more flexible architecture of parallel processing (23), but it is also in keeping with recent functional neuroimaging findings (8, 16, 24) and contemporary models of language disorders (5, 23, 25). The current study focused on the lateralization of these pathways and possible behavioral advantages related to the degree of lateralization.

Results

First, we obtained DT-MRI brain scans of 50 healthy right-handed subjects (30 males and 20 females) with a 1.5-T GE scanner, using an acquisition sequence fully optimized for DT-MRI of white matter and coverage of the whole head (26). Then we adopted a two-step approach to brain dissections. The first step consisted of creating an average template from DT-MRI data sets of 10 male subjects as described in Jones *et al.* (27). In

Author contributions: M.C., M.P.G.A., M.H., M.M.M., and R.M.M. designed research; M.C., M.P.G.A., L.P., and D.K.J. performed research; M.C., M.P.G.A., L.P., and D.K.J. contributed new reagents/analytic tools; M.C., M.H., L.P., and D.K.J. analyzed data; and M.C., M.P.G.A., M.H., L.P., M.M.M., R.M.M., and D.K.J. wrote the paper.

The authors declare no conflict of interest.

This article is a PNAS Direct Submission.

Abbreviations: DT, diffusion tensor; CVLT, California Verbal Learning Test; ROI, region of interest.

§To whom correspondence should be addressed. E-mail: m.catani@iop.kcl.ac.uk.

This article contains supporting information online at www.pnas.org/cgi/content/full/0702116104/DC1.

NEUROSCIENCE

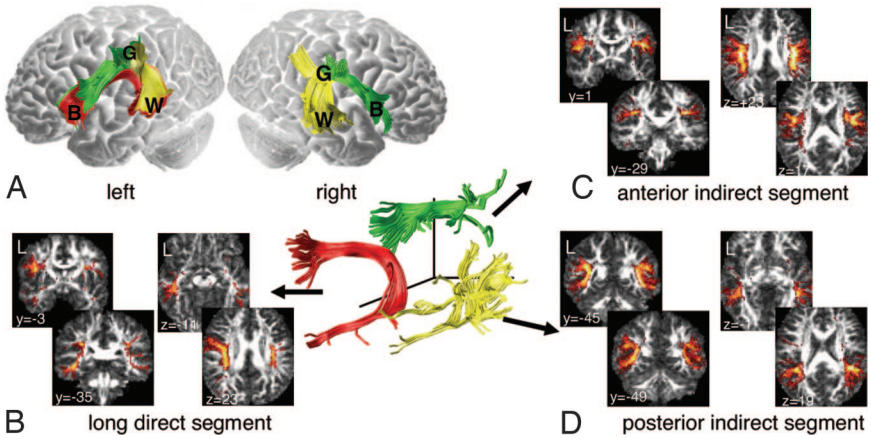

Fig. 1. Left–right hemispheric differences in perisylvian language pathways. (*A*) Tractography reconstruction of language pathways in the average DT-MRI data set. In both hemispheres, the anterior indirect segment (green) connects posterior inferior frontal cortex (B, Broca's territory) and inferior parietal cortex (G, Geschwind's territory), whereas the posterior indirect segment (yellow) connects superior posterior temporal cortex (W, Wernicke's territory) and Geschwind's territory. In the left hemisphere, but not in the right, the direct segment (red) connects Wernicke's and Broca's territories. (*B–D*) Segment overlap maps derived from dissection of single brains show L-R asymmetry only in the direct segment (*B*) and L-R symmetry in the anterior indirect (*C*) and posterior indirect (*D*) segments. ''Hotter'' (yellow) colors correspond to a higher degree of overlap, whereas ''cooler'' (red) colors reflect less overlap.

each hemisphere, virtual dissections of the three segments of the perisylvian language networks were performed for the average brain (21). Then, to confirm the exploratory analysis derived from dissections of the average brain, similar dissections were performed in each of the remaining 40 single subjects.

Asymmetry of Perisylvian Language Networks. The reconstruction of the perisylvian language networks in the average DT-MRI data set indicates an asymmetrical representation, with a very different connection pattern in the left hemisphere compared with the right (Fig. 1*A*). Critically, although the indirect pathway is represented in both hemispheres, consisting of an anterior indirect segment (denoted in green in Fig. 1*A*) and a posterior indirect segment (denoted in yellow in Fig. 1*A*), it was not possible to reconstruct pathways directly connecting frontal and temporal regions in the right hemisphere of the average data set. Only the left hemisphere reconstructions contain a direct segment (denoted in red in Fig. 1*A*).

Although these findings suggest differences in language networks between the left and right hemispheres, they were derived from an averaged DT-MRI data set. Of critical importance is whether such asymmetries are observed in individual subjects. We therefore performed individual dissections on the data acquired from 40 subjects and created, for each segment, maps showing the overlap of the segment from each subject. The segment overlap maps derived from the single brain dissections confirm the asymmetrical distribution of the direct segment (Fig. 1*B*) and the symmetrical distribution of the anterior indirect (Fig. 1*C*) and posterior indirect (Fig. 1*D*) segments. [The complete series of the segment overlap maps can be seen in supporting information (SI) Fig. 3.]

The segment-overlap maps give an overall idea of the interhemispheric distribution of the number of reconstructed pathways but may underestimate the heterogeneity within the sample studied. For this reason, a lateralization index was calculated by counting the number of reconstructed pathways within the direct segment for each hemisphere. To facilitate a visual representation of the heterogeneous distribution, a *k*-means cluster analysis was performed to broadly classify the data sets into three groups (Fig. 2*A*). This procedure makes no assumptions about underlying differences between individuals but attempts to objectively identify relatively homogeneous groups of cases. The cluster analysis showed that 62.5% (25/40) of the subjects presented an extreme left lateralization of the direct segment (cluster center of the lateralization index = 1.93) (Group 1). In the majority of subjects in Group 1, it was not possible to reconstruct a continuous trajectory between equivalents of Broca's and Wernicke's territories in the right hemisphere. Another 20% (8/40) of all of the subjects demonstrated leftward asymmetries but with some representation of the right direct segment in the reconstructed pathways (cluster center of the lateralization index = 1.03); thus they had a bilateral but leftward asymmetric distribution (Group 2). Only 17.5% (7/40) of the subjects had similar left-right distribution (cluster center of the lateralization index = 0.03) (Group 3).

Further, for each subject, we obtained the mean value of the fractional anisotropy sampled along each tract segment, which we term ''tract-specific measurement'' (28). Fractional anisotropy is a scalar measure that reflects the degree to which the diffusivity depends on the orientation in which it is measured (changes in which are thought to reflect changes in tissue microstructure) and therefore considered an index of microstructural ordering and integrity of fibers. Interhemispheric differences were found in the fractional anisotropy, with values of the anterior indirect segment (left, 0.445 ± 0.024; right, 0.465 ± 0.023; $P = 0.001$) and, to a lesser degree, the direct segment (left, 0.488 ± 0.024; right, 0.475 ± 0.029; $P = 0.048$) being significantly different between the left and right sides. Also, for each subject and segment, a lateralization index of the fractional anisotropy values was calculated (SI Fig. 4). A rightward distribution of the fractional anisotropy lateralization index of the anterior indirect segment (mean ratio = −0.03 ± 0.64; $P = 0.002$) and a leftward distribution of the fractional anisotropy index of the direct segment (mean ratio 0.03 ± 0.073; $P = 0.035$) were found.

Patterns of Lateralization and Behavioral Correlates. A significant positive correlation was found between the lateralization index of reconstructed pathways in the direct segment and the performances in the California Verbal Learning Test (CVLT; total words recall) (Pearson's correlation 0.564, $P < 0.001$; correlations are significant at $P < 0.005$ after Bonferroni correction) (Fig. 2*B*). The CVLT consists of five learning trials of a 16-word list. The list is read aloud by the examiner, and the examinee is instructed to freely recall as many words as possible, in any order. Each of the 16 words belongs to one of four categories of ''shopping list'' items (i.e., fruits, herbs and spices, articles of clothing and of tools). The idea underlying the

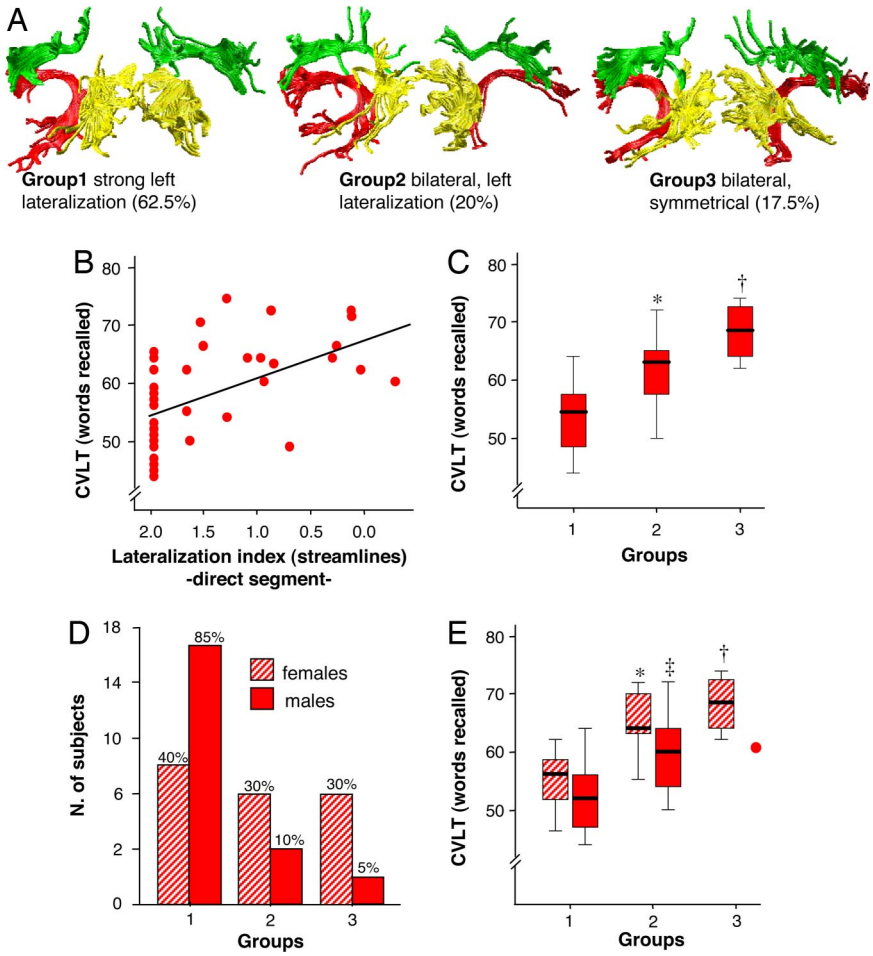

Fig. 2. Lateralization of language pathways and behavioral correlates. (*A*) Distribution of the lateralization pattern of the direct long segment (red). (*B*) Significant correlation between the lateralization index (streamlines) of the direct segment and performances on the CVLT (number of words correctly recalled of 80). (*C*) Performances in the CVLT according to the three lateralization groups (*, $P < 0.01$ vs. Group 1; †, $P < 0.001$ vs. Group 1). (*D*) Distribution of the lateralization groups between genders. (*E*) Performances in the CVLT according to the lateralization pattern and gender (striped colors are females) (*, $P < 0.05$ vs. Group 1; †, $P < 0.01$ vs. Group 1; ‡, $P < 0.05$ vs. Group 1).

CVLT is that lists of words are easier to remember if they are broken down by using a strategy of grouping them into semantic categories. After the first trial, the same 16-word list is reread aloud by the examiner, and the examinee is asked to recall again as many words as possible. The same procedure is used for the remaining three trials. Overall, total recall (i.e., the number of words correctly recalled of 80) was lower for subjects with extreme left lateralization (Group 1) (53.5 ± 6) than for those with bilateral, symmetrical (Group 3) (68.2 ± 5.3; $P < 0.001$), or asymmetrical patterns (Group 2) (61.7 ± 7; $P < 0.01$) (Fig. 2*C*). Thus, a more symmetrical pattern was associated with better performance on the CVLT. There were no significant differences among the three groups in performance on any of the other neuropsychological tests performed.

Gender Differences in the Lateralization Pattern. A preliminary analysis was performed to assess gender differences in the anatomy of perisylvian language pathways. Fig. 2*D* shows the difference in the distribution of lateralization pattern between the two genders (Fisher's exact test = 8.496; $P = 0.018$). Overall, males showed a greater leftward lateralization (mean lateralization index = 1.52 ± 0.64) compared with females (mean lateralization index = 1.07 ± 0.72) ($P < 0.05$). Despite the anatomical differences, both genders showed a significant correlation between the pattern of lateralization of the direct segment and the performances in the CVLT (Fig. 2*E*). Thus in males, Group 1 performed worse than Group 2 ($P < 0.05$); in females, Group1 performed worse than Group 2 ($P < 0.05$) and Group 3 ($P < 0.01$).

There were no differences between the genders (SI Table 1) in the lateralization index of the fractional anisotropy values and no correlation between the fractional anisotropy values and neuropsychological performances after correction for multiple comparisons (SI Table 2).

Discussion

DT-MRI tractography is the only technique that allows the identification of large pathways and assessment of microstructural integrity of white matter in the living human brain (29). Hence, we used DT-MRI tractography to look for correlation between symmetries within white matter of the language system and behavioral performances.

Previous studies have shown direct correspondence between tractography-derived anatomy of white matter pathways and classical postmortem descriptions (30, 31). Nevertheless, it is important to note that DT-MRI tractography offers, at best, only indirect indices of tissue properties, and therefore there is uncertainty in the correspondence between tractography measurements (e.g., number of reconstructed pathways) and underlying biological factors (e.g., number of axons, degree of myelination, etc.). We therefore do not assume that our findings are

equivalent to data obtained from postmortem dissections, although they are likely to reflect highly reproducible features of the human brain anatomy.

Converging evidence of the existence of the three perisylvian segments derives from human intraoperative electrocorticography (32), functional connectivity (33), and postmortem dissections (34), and there is also some evidence of a rudimentary homologue of the three segments in the monkey (35). However, none of the previous studies were concerned with interhemispheric differences and the correlation between lateralization of pathways and language function.

Three important findings emerge from this study. First, the white matter anatomy of perisylvian language networks differs between the two hemispheres. Second, the pattern of lateralization is heterogeneous in the normal population. Finally, bilateral representation of language networks is associated with better performance in learning words by semantic association.

The overall prevalence of asymmetrical distribution of the direct segment of the arcuate fasciculus in our right-handed population is higher (82.5%) than that reported for the planum temporale (65%), the region of the posterior superior temporal gyrus classically associated with language lateralization (4). Considering that the prevalence of left functional "dominance" for language is >90% (9, 10), asymmetry of the direct segment may represent a key anatomical substrate for language lateralization.

In general, our findings are consistent with previous neuroimaging studies showing structural (11, 12, 22, 36, 37) and maturational (38) differences of the arcuate fasciculus between left and right hemispheres. However, the existence of an arcuate fasciculus in the right human brain has never been confirmed in postmortem studies and, to the best of our knowledge, such a strong relationship between brain pathway architecture and cognitive performance has never previously been described. The CVLT assesses encoding and retrieval of a list of auditorily presented words. Because each word in the list can be categorized in one of the four "shopping list" groups and can therefore be clustered together with other semantically associated words, the CVLT is considered a test that does not examine verbal memory in itself, but rather some level of interaction between verbal memory and conceptual ability (39). The CVLT is a complex cognitive task that is known to require additional involvement of the right hemisphere as shown by fMRI in subjects performing the test (17). Our data suggest that direct connections between inferior frontal and posterior temporal regions in the right hemisphere confer an advantage for the performance of this task. This finding is supportive of the role of the right hemisphere in word retrieval (40) and in keeping with evolutionary theories of the effects of brain lateralization on human cognition (41). On the other hand, we did not find correlations with other language functions that were tested in the study group. It is possible that some of the linguistic tasks we have tested may correlate with other tracts that were not analyzed in our study or alternatively may be not specific to any single anatomical structure. Verbal fluency, for example, is associated with lesions of an extended network connecting lateral to medial frontal cortex and the head of caudate, a network that is not part of the perisylvian circuitry (5).

A preliminary analysis of the data also suggests gender differences on the large-scale anatomy of language pathways but no differences at the microstructural level (i.e., males and females had similar lateralization indices of fractional anisotropy). Some studies have shown gender differences in language cortical (42) and subcortical anatomy (11), activation patterns on linguistic tasks (43), and cognitive performances (44), whereas other studies showed no differences (45). Here, we found that the female group had lower lateralization of the direct segment and slightly better performances in the CVLT compared with males (SI Table 3). Kramer *et al.* (46) have demonstrated that females tend to outperform males on recall measures of this test. However, our findings of better performances of Group 2 over Group 1 in both genders (Fig. 2*E*) support the notion that the main determinant of better performance is the anatomy (i.e., symmetry) of the language pathways, not the gender.

In conclusion, our data suggest the relationship between functional and anatomical lateralization might not be as straightforward as previously believed. Our findings not only show hemispheric differences in connections between inferior frontal and posterior temporal regions but also critically suggest that individuals with more symmetric patterns of connection are better overall at learning words using semantic association. The correlation between anatomical lateralization and neuropsychological performances brings up interesting hypotheses on possible anatomical predictors of aphasia recovery that can be tested in patients with lesions of perisylvian language networks.

Experimental Procedures

Study Participants. Data sets from 10 male subjects (mean age = 33.3 ± 4.7 years) were used to create an average tensor data set as described in Jones *et al.* (27) (see below). Data sets from 40 additional subjects (20 males and 20 females, age range 18–22 years) were used to perform single dissections of the three language segments and create segment overlap maps. All subjects were right-handed healthy individuals. Approval was obtained from the Joint Medical Ethical Committee of the Institute of Psychiatry, Kings College London. Informed written consent was obtained from all participants.

Neuropsychological Testing. The neuropsychological testing (SI Table 3) included: the Wechsler Abbreviated Scale of Intelligence; block design and matrices as subtests for performance IQ and vocabulary and similarities for performance IQ (47); the Controlled Oral Word Association Test (to test phonological and semantic verbal fluency) (48); the Hayling Sentence Completion Task (a test of verbal initiation and inhibition) (49); the CVLT (to assess the use of semantic associations as strategy for learning words) (50); and the Wechsler Memory Scale (immediate and delayed recall of geometric shapes) (51). Handedness was assessed by using the Edinburgh Handedness Inventory (52).

DT-MRI Acquisition. Data were acquired on a GE Signa 1.5-T LX MRI system (General Electric, Milwaukee, WI) with 40-mT/m gradients, using an acquisition sequence fully optimized for DT-MRI of white matter, providing isotropic resolution (2.5 × 2.5 × 2.5 mm) and coverage of the whole head. The acquisition was gated to the cardiac cycle by using a peripheral gating device placed on the subjects' forefinger. Full details of the acquisition sequence are provided in Jones *et al.* (26).

After correction for the image distortions introduced by the application of the diffusion encoding gradients, the DT was determined in each voxel following the method of Basser *et al.* (53). After diagonalization of the DT, the fractional anisotropy (54) was measured in each voxel. To ensure that the observer was blind to hemisphere during the virtual dissection of the language pathways and therefore to provide protection against subjective bias, half of the DT-MRI data sets were reflected about the midline.

Averaging of DT-MRI Data Sets. DT-MRI data sets from 10 male subjects were spatially normalized to the anatomical reference space defined by the Montreal Neurological Institute Echo Planar Imaging (MNI EPI) template supplied as part of the of the functional imaging analysis software package SPM99 (statistical parametric mapping; Wellcome Department of Cognitive Neurology, London, U.K.). The use of the male average brain was preferred for consistency with our previous findings, where we described the three segments for the first time in the left hemisphere of 10 male subjects (21). For each of the 10 source

subjects, the masked tensor volume data set was coregistered (using an affine registration with 12 degrees of freedom) to the template using the approach described by Alexander *et al.* (55). This approach uses the Automated Image Registration (AIR) registration package (56, 57) for coregistration, and the computed transformations thus obtained are applied to the DT-MRI volumes using the preservation of principal directions algorithm (55), which has been shown to reorient each tensor correctly under nonrigid transformations. The images used for coregistration were the fractional anisotropy images computed from the six elements of the tensor (54). Full details of the spatial normalization procedure and generation of an average DT-MRI volume are described in Jones *et al.* (27).

Tractography Algorithm. The software for reconstructing the trajectories of tracts from DT data were written in the "C" programming language and based on the procedure originally described by Basser *et al*. (58). Details of the method have been published (21, 30), but a brief description will follow. First, a continuous description of the DT field was derived from the voxel-wise discrete estimates by B-spline fitting a series of basis functions to the elements of the tensor matrices (58). This procedure allows rapid evaluation of the DT at any arbitrary location within the imaged volume and also permits smoothing of the tensor field. A set of locations for the initiation of the tracking algorithm (the "seed-points") was first selected on the fractional anisotropy images (see below). For each of these seed-points, the DT was estimated and diagonalized to determine the principal eigenvector. The tracking algorithm then moved a distance of 0.5 mm along this direction. The DT was determined at this new location (obtained from the continuous description of the tensor field) and the orientation of its principal eigenvector estimated. The algorithm then moved a further 0.5 mm along this new direction. A pathway was traced out in this manner until the fractional anisotropy of the tensor fell below a fixed arbitrary threshold (set to 0.2). The procedure was then repeated by tracking in the opposite direction, to reconstruct the whole tract passing through the seed-point.

At the termination of tracking, the number of reconstructed pathways and the fractional anisotropy, which quantifies the directionality of diffusion on a scale from zero (when diffusion is totally random) to one (when water molecules are able to diffuse along one direction only), was sampled at regular (0.5-mm) intervals along the tract and the means computed (28). For each reconstructed segment, a lateralization index was calculated according to the following formula (N., number):

$$\frac{(\text{N. streamlines-left}) - (\text{N. streamlines-right})}{[(\text{N. streamlines-left}) + (\text{N. streamlines-right})]/2}.$$

Positive values of the index indicate a greater number of streamlines in the left direct segment compared with the right. Values around the zero indicate a similar number of streamlines between left and right. Similarly, a lateralization index was calculated for the fractional anisotropy values of each segment.

Virtual Dissections of the Language Networks and Segment Overlap Maps. SI Fig. 5 shows the method used to perform virtual dissections of the left and right perisylvian connections between frontal, parietal, and temporal regions (21). A region of interest (ROI) was defined on the axial fractional anisotropy map computed from the average DT-MRI volume, to encompass the horizontal fibers lateral to the corona radiata and medial to the cortex extending from Talairach $z = 22$ to $z = 28$. All fibers passing through this ROI were reconstructed in three dimensions by using MATLAB (Mathworks, Natick, MA) and visualized as illuminated streamtubes. The ROI was defined on axial slices as this projection facilitates the visualization of the borders between the fibers of the arcuate and those of the corona radiata. A two-ROI approach was used to perform further detailed dissection of the arcuate fasciculus, allowing us to separate different sets of fibers within the arcuate bundle. Here, two spatially separated regions are defined in the fractional anisotropy volume, and all fibers passing through both are visualized as described above. The approach does not constrain tracts to start and end within the defined regions, only to pass through them. The distribution of arcuate fiber terminations found by tractography extends beyond the classical limits of Broca's and Wernicke's areas to include in addition to the inferior frontal cortex part of the middle frontal gyrus and in addition to the superior temporal cortex the posterior middle temporal gyrus respectively. For this reason, we refer to these extended regions as Broca's and Wernicke's territories (21). The delineation of regions used in two-ROI dissections was guided by the results of the one-ROI dissection. The single segments were visually inspected for the presence of aberrant streamlines (e.g., streamlines leaving the arcuate fasciculus and projecting into the internal capsule) and anatomical correspondence between the two hemispheres. The number of seeds use to start tracking was similar between the two hemispheres, and none of the subjects showed aberrant fibers within the direct segment when the two-ROI approach was used.

For each subject and segment, a binary map with dimensions equal to that of the DT-MRI data (i.e., $128 \times 128 \times 60$) was computed by assigning each pixel a value of 1 or 0 depending on whether the pixel was intersected by the tract segment. For each segment, the binary maps from all 40 subjects were spatially normalized to the fractional anisotropy map derived from the average tensor data set, and the maps summed to produce segment overlap maps on axial, sagittal, and coronal slices (SI Fig. 3). Finally, a second operator defined ROIs in a randomly selected sample of 10 subjects, and interrater reliability was calculated for the long segment (correlation 0.93 for the lateralization index of the number of streamlines and 0.99 for the fractional anisotropy measurements).

Statistical Analysis. Statistical analysis was performed by using SPSS software (SPSS, Chicago, IL). Subjects were clustered into three groups according to the left-right distribution of the reconstructed pathways of the direct segment using a *k*-means cluster analysis (59). χ^2 (or Fisher's exact test) was used to assess the distribution of the lateralization index across the subjects and between genders. One-sample *t* test (test value = 0) was used to assess the lateralization of the index of the fractional anisotropy values and two-way ANOVA for between-genders differences (SI Table 1). Correlation analysis was performed between the lateralization index of the direct segment (streamlines) and the neuropsychological performances (correlations are significant at $P < 0.005$ after Bonferroni correction for multiple comparisons). Also, correlation analysis was performed between tract-specific measurements of fractional anisotropy and neuropsychological performances (correlations are significant at $P < 0.0016$ after Bonferroni correction for multiple comparisons). ANOVA was used to account for gender differences in handedness and neuropsychological performances (SI Table 3). Two-way ANOVA was used to assess differences in neuropsychological performances among the three groups. Interrater reliability for the lateralization index of the long segment was 0.93 for the number of streamlines and 0.99 for the fractional anisotropy measurements.

We thank Cathy Price and Marion Cuddy for comments on the manuscript. This research was funded by the Medical Research Council (U.K.), the AIMS network, the Wellcome Trust, and the Psychiatry Research Trust. M.P.G.A. is a Peggy Pollak Research Fellow in Developmental Psychiatry.

1. Geschwind N, Galaburda AM (1985) *Arch Neurol* 42:428–459.
2. Gannon PJ, Holloway RL, Broadfield DC, Braun AR (1998) *Science* 279:220–222.
3. Nottebohm F (1970) *Science* 167:950–956.
4. Geschwind N, Levitsky W (1968) *Science* 161:186–187.
5. Damasio H, Damasio A (2000) in *Principles of Behavioural and Cognitive Neurology*, ed Mesulam M (Oxford Univ Press, New York), pp 294–315.
6. Gazzaniga MS (1995) *Neuron* 14:217–228.
7. Mesulam M (2000) in *Principles of Behavioural and Cognitive Neurology*, ed Mesulam M (Oxford Univ Press, New York), pp 1–120.
8. Stephan KE, Marshall JC, Friston KJ, Rowe JB, Ritzl A, Zilles K, Fink GR (2003) *Science* 301:384–386.
9. Toga AW, Thompson PM (2003) *Nat Rev Neurosci* 4:37–48.
10. Dorsaint-Pierre R, Penhune VB, Watkins KE, Neelin P, Lerch JP, Bouffard M, Zatorre RJ (2006) *Brain* 129:1164–1176.
11. Hagmann P, Cammoun L, Martuzzi R, Maeder P, Clarke S, Thiran JP, Meuli R (2006) *Hum Brain Mapp* 27:828–835.
12. Nucifora PG, Verma R, Melhem ER, Gur RE, Gur RC (2005) *NeuroReport* 16:791–794.
13. Parker GJ, Luzzi S, Alexander DC, Wheeler-Kingshott CA, Ciccarelli O, Lambon Ralph MA (2005) *NeuroImage* 24:656–666.
14. Penhune VB, Zatorre RJ, MacDonald JD, Evans AC (1996) *Cereb Cortex* 6:661–672.
15. Fletcher PC, Frith CD, Grasby PM, Shallice T, Frackowiak RS, Dolan RJ (1995) *Brain* 118:401–416.
16. Jung-Beeman M (2005) *Trends Cognit Sci* 9:512–518.
17. Johnson SC, Saykin AJ, Flashman LA, McAllister TW, Sparling MB (2001) *J Int Neuropsychol Soc* 7:55–62.
18. Damasio H, Tranel D, Grabowski T, Adolphs R, Damasio A (2004) *Cognition* 92:179–229.
19. Devlin JT, Moore CJ, Mummery CJ, Gorno-Tempini ML, Phillips JA, Noppeney U, Frackowiak RS, Friston KJ, Price CJ (2002) *NeuroImage* 15:675–685.
20. Barrick TR, Lawes IN, Mackay CE, Clark CA (2007) *Cereb Cortex* 17:591–598.
21. Catani M, Jones DK, ffytche DH (2005) *Ann Neurol* 57:8–16.
22. Powell HW, Parker GJ, Alexander DC, Symms MR, Boulby PA, Wheeler-Kingshott CA, Barker GJ, Noppeney U, Koepp MJ, Duncan JS (2006) *NeuroImage* 32:388–399.
23. Mesulam M (2005) *Ann Neurol* 57:5–7.
24. Sakai KL (2005) *Science* 310:815–819.
25. Catani M, ffytche DH (2005) *Brain* 128:2224–2239.
26. Jones DK, Williams SC, Gasston D, Horsfield MA, Simmons A, Howard R (2002) *Hum Brain Mapp* 15:216–230.
27. Jones DK, Griffin LD, Alexander DC, Catani M, Horsfield MA, Howard R, Williams SC (2002) *NeuroImage* 17:592–617.
28. Jones DK, Catani M, Pierpaoli C, Reeves SJ, Shergill SS, O'Sullivan M, Golesworthy P, McGuire P, Horsfield MA, Simmons A, *et al.* (2006) *Hum Brain Mapp* 27:230–238.
29. Le Bihan D (2003) *Nat Rev Neurosci* 4:469–480.
30. Catani M, Howard RJ, Pajevic S, Jones DK (2002) *NeuroImage* 17:77–94.
31. Wakana S, Caprihan A, Panzenboeck MM, Fallon JH, Perry M, Gollub RL, Hua K, Zhang J, Jiang H, Dubey P, *et al.* (2007) *NeuroImage* 36:630–644.
32. Matsumoto R, Nair DR, LaPresto E, Najm I, Bingaman W, Shibasaki H, Luders HO (2004) *Brain* 127:2316–2330.
33. Schmithorst VJ, Holland SK (2007) *NeuroImage* 35:406–419.
34. Lawes IN, Barrick TR, Murugam V, Spierings N, Evans D, Song M, Clark CA (2007) *NeuroImage*, in press.
35. Deacon TW (1992) *Brain Res* 573:8–26.
36. Buchel C, Raedler T, Sommer M, Sach M, Weiller C, Koch MA (2004) *Cereb Cortex* 14:945–951.
37. Galuske RA, Schlote W, Bratzke H, Singer W (2000) *Science* 289:1946–1949.
38. Paus T, Zijdenbos A, Worsley K, Collins DL, Blumenthal J, Giedd JN, Rapoport JL, Evans AC (1999) *Science* 283:1908–1911.
39. Lezak MD, Howieson DB, Loring DW (2004) *Neuropsychological Assessment* (Oxford Univ Press, Oxford).
40. Habib R, Nyberg L, Tulving E (2003) *Trends Cognit Sci* 7:241–245.
41. Corballis PM, Funnell MG, Gazzaniga MS (2000) *Brain Cognit* 43:112–117.
42. Luders E, Narr KL, Thompson PM, Rex DE, Jancke L, Steinmetz H, Toga AW (2004) *Nat Neurosci* 7:799–800.
43. Shaywitz BA, Shaywitz SE, Pugh KR, Constable RT, Skudlarski P, Fulbright RK, Bronen RA, Fletcher JM, Shankweiler DP, Katz L, *et al.* (1995) *Nature* 373:607–609.
44. Baron-Cohen S, Knickmeyer RC, Belmonte MK (2005) *Science* 310:819–823.
45. Sommer IE, Aleman A, Bouma A, Kahn RS (2004) *Brain* 127:1845–1852.
46. Kramer JH, Delis DC, Daniel M (1988) *J Clin Psychol* 44:907–915.
47. Wechsler D (1999) *Wechsler Abbreviated Scale of Intelligence* (Psychological Corporation, New York).
48. Benton AL, Hamsher KdS (1976) *Multilingual Aphasia Examination* (University of Iowa, Iowa City).
49. Burgess PW, Shallice T (1997) *The Hayling and Brixton Tests* (Thames Valley Test Co, Suffolk, UK).
50. Delis DC, Kramer JH, Kaplan E, Ober BA (1987) *CVLT: Californian Verbal Learning Test* (Psychological Corporation, New York).
51. Wechsler D (1987) *Wechsler Memory Scale-Revised* (Psychological Corporation, San Antonio, TX).
52. Oldfield RC (1971) *Neuropsychologia* 9:97–113.
53. Basser PJ, Mattiello J, LeBihan D (1994) *Biophys J* 66:259–267.
54. Basser PJ, Pierpaoli C (1996) *J Magn Reson B* 111:209–219.
55. Alexander DC, Pierpaoli C, Basser PJ, Gee JC (2001) *IEEE Trans Med Imaging* 20:1131–1139.
56. Woods RP, Grafton ST, Holmes CJ, Cherry SR, Mazziotta JC (1998) *J Comput Assist Tomogr* 22:139–152.
57. Woods RP, Grafton ST, Watson JD, Sicotte NL, Mazziotta JC (1998) *J Comput Assist Tomogr* 22:153–165.
58. Basser PJ, Pajevic S, Pierpaoli C, Duda J, Aldroubi A (2000) *Magn Reson Med* 44:625–632.
59. Aldenderfer MS, Blashfield RK (1984) *Cluster Analysis* (Sage Publications, Newbury Park, CA).